

Supporting Information

Silicon-Doped Argyrodite Solid Electrolyte $\text{Li}_6\text{PS}_5\text{I}$ with Improved Ionic Conductivity and Interfacial Compatibility for High-Performance All-Solid-State Lithium Batteries

*Jun Zhang,[‡] Lujie Li,[‡] Chao Zheng, Yang Xia, Yongping Gan, Hui Huang, Chu Liang, Xinpeng He,
Xinyong Tao and Wenkui Zhang**

College of Materials Science and Engineering, Zhejiang University of Technology, Hangzhou
310014, P.R. China.

[‡]J. Zhang and L. Li contributed equally to this work.

*Corresponding author. E-mail: msechem@zjut.edu.cn

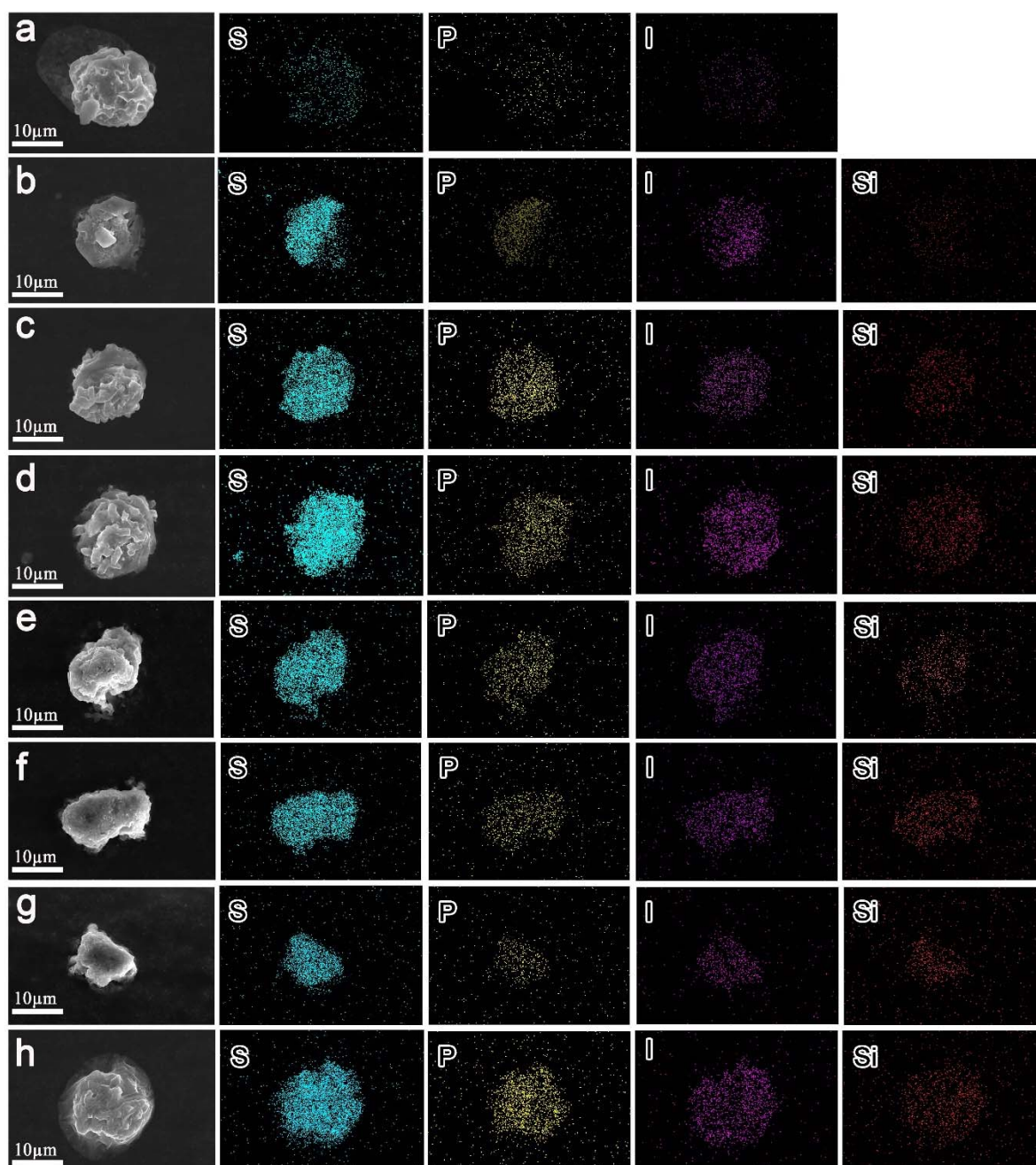


Figure S1. SEM images of (a) $\text{Li}_6\text{PS}_5\text{I}$, (b-h) $\text{Li}_{6+x}\text{P}_{1-x}\text{Si}_x\text{S}_5\text{I}$ ($0.1 \leq x \leq 0.6$) powders and the corresponding element mapping.

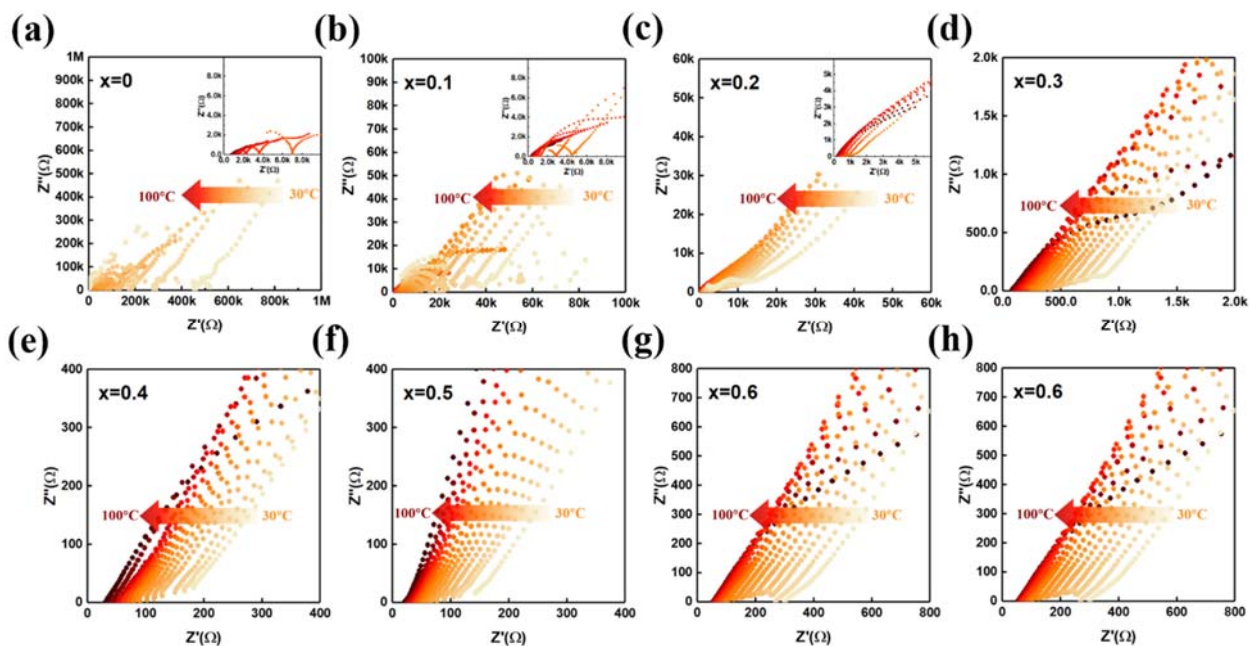


Figure S2. Nyquist plots of the (a) $\text{Li}_6\text{PS}_5\text{I}$ ($x = 0$), (b-h) $\text{Li}_{6+x}\text{P}_{1-x}\text{Si}_x\text{S}_5\text{I}$ ($0.1 \leq x \leq 0.6$) samples measured from 30 °C to 100 °C, respectively.

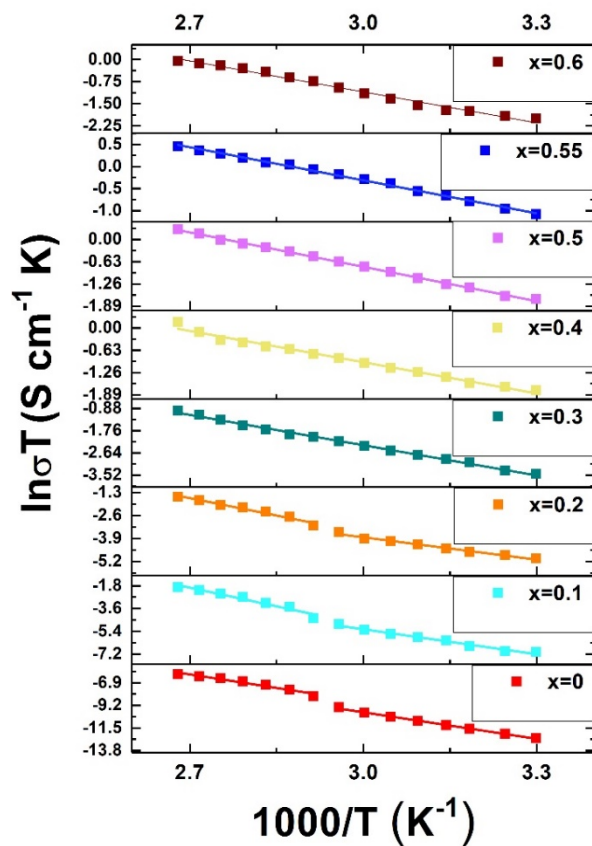


Figure S3. Arrhenius curves for activation energy of $\text{Li}_{6+x}\text{P}_{1-x}\text{Si}_x\text{S}_5\text{I}$ ($0 \leq x \leq 0.6$) samples.

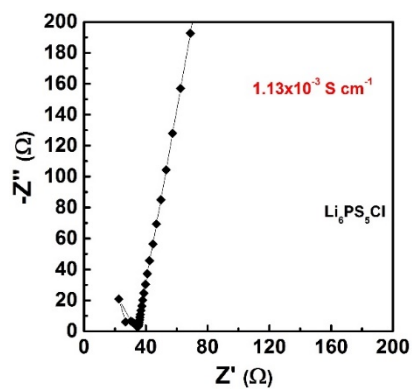


Figure S4. Nyquist plots of $\text{Li}_6\text{PS}_5\text{Cl}$ sample measured at 30 °C.

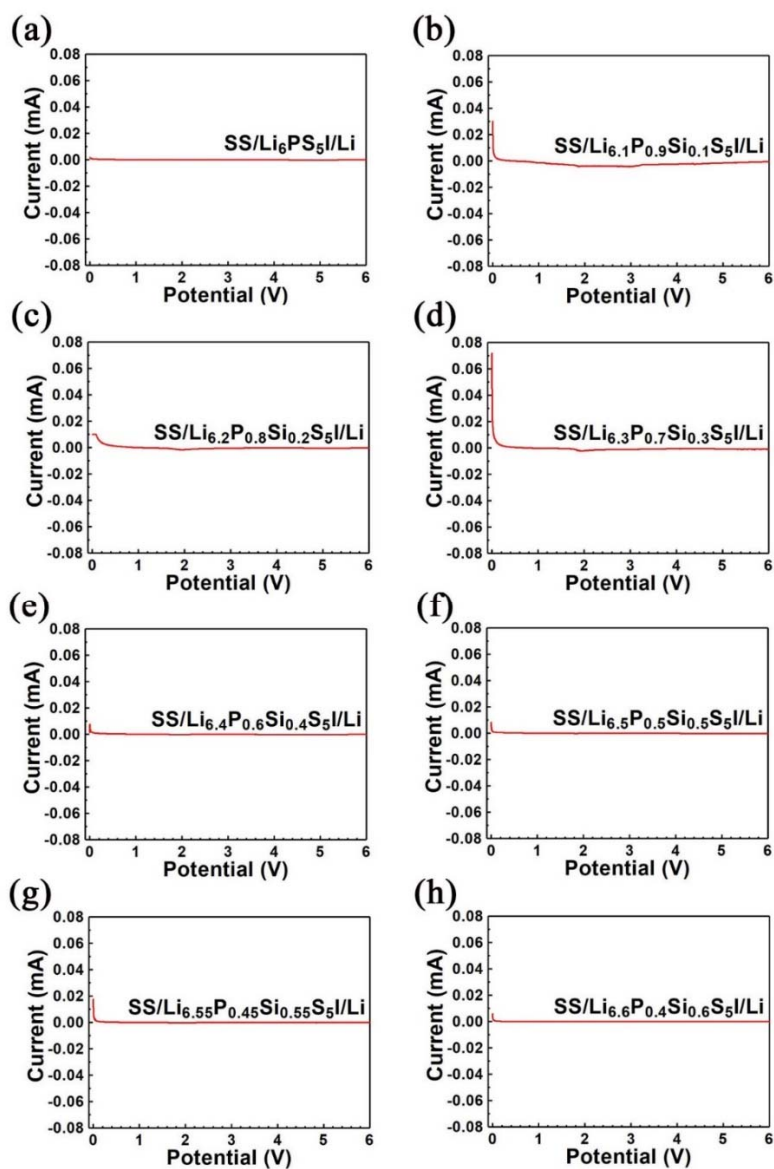


Figure S5. Linear sweep voltammogram (LSV) profile of (a) $\text{Li}_6\text{PS}_5\text{I}$, (b-h) $\text{Li}_{6+x}\text{P}_{1-x}\text{Si}_x\text{S}_5\text{I}$ ($0.1 \leq x \leq 0.6$) samples at a scan rate of 0.1 mV s^{-1} , respectively.

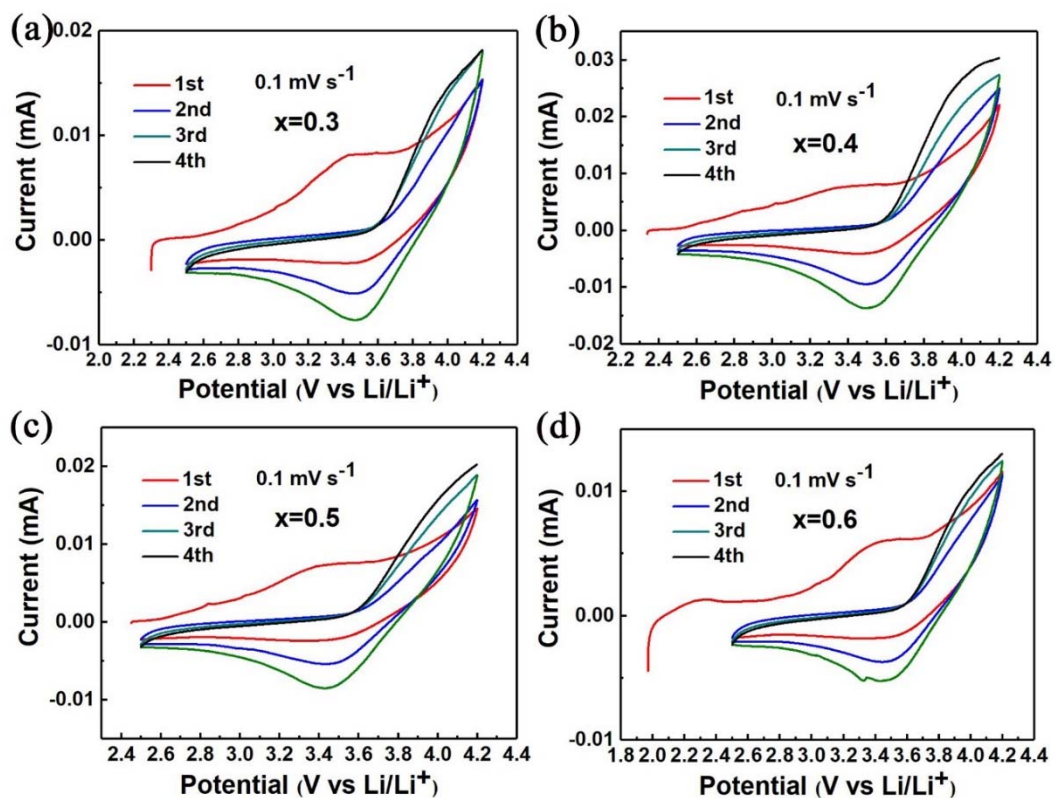


Figure S6. CV curves of the (a-d) $\text{Li}_{6+x}\text{P}_{1-x}\text{Si}_x\text{S}_5\text{I}$ ($0.3 \leq x \leq 0.6$) of NCM- $\text{Li}_6\text{PS}_5\text{Cl}$ / $\text{Li}_{6+x}\text{P}_{1-x}\text{Si}_x\text{S}_5\text{I}$ / Li ASSLBs at a scan rate of 0.1 mV s^{-1} .

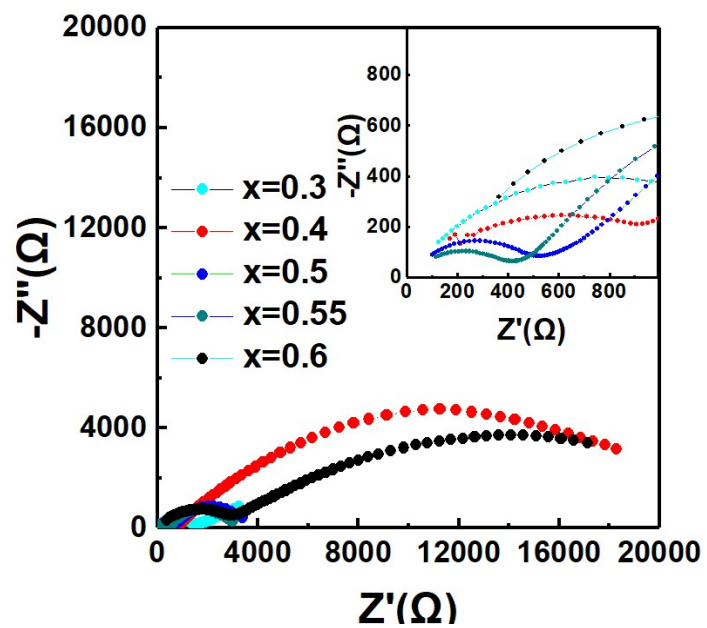


Figure S7. Impedance spectra of NCM-Li₆PS₅Cl/ Li_{6+x}P_{1-x}Si_xS₅I (x = 0.3, 0.4, 0.5 and 0.6)/ Li ASSLBs after 300 cycles.

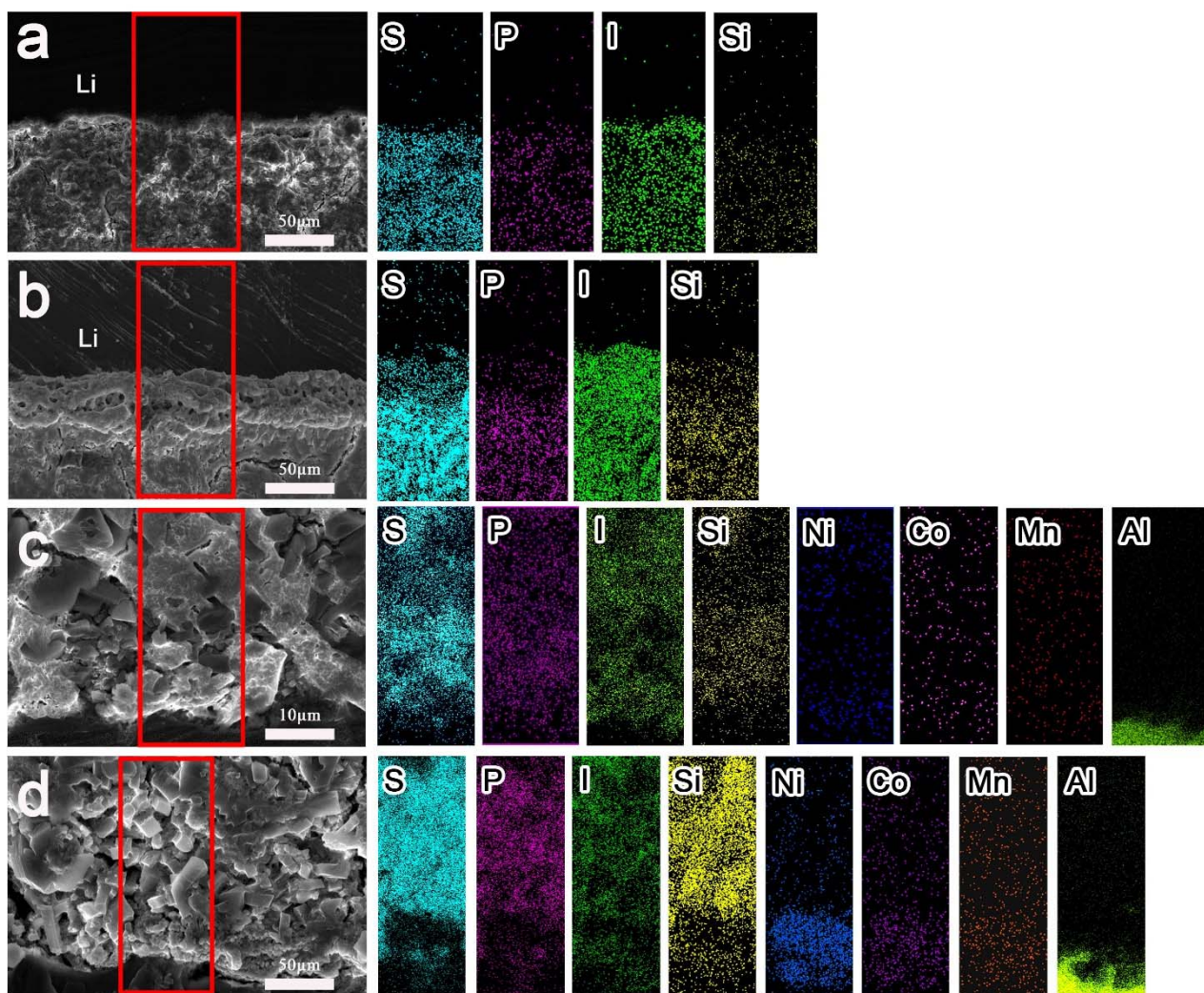


Figure S8. The cross-sectional SEM images and the corresponding elemental mappings of the interface of $\text{Li}_{6.55}\text{P}_{0.45}\text{Si}_{0.55}\text{S}_5\text{I}$ SE/Li before (a) and after cycling (b); $\text{Li}_{6.55}\text{P}_{0.45}\text{Si}_{0.55}\text{S}_5\text{I}$ SE/NCM before (c) and after cycling (d).

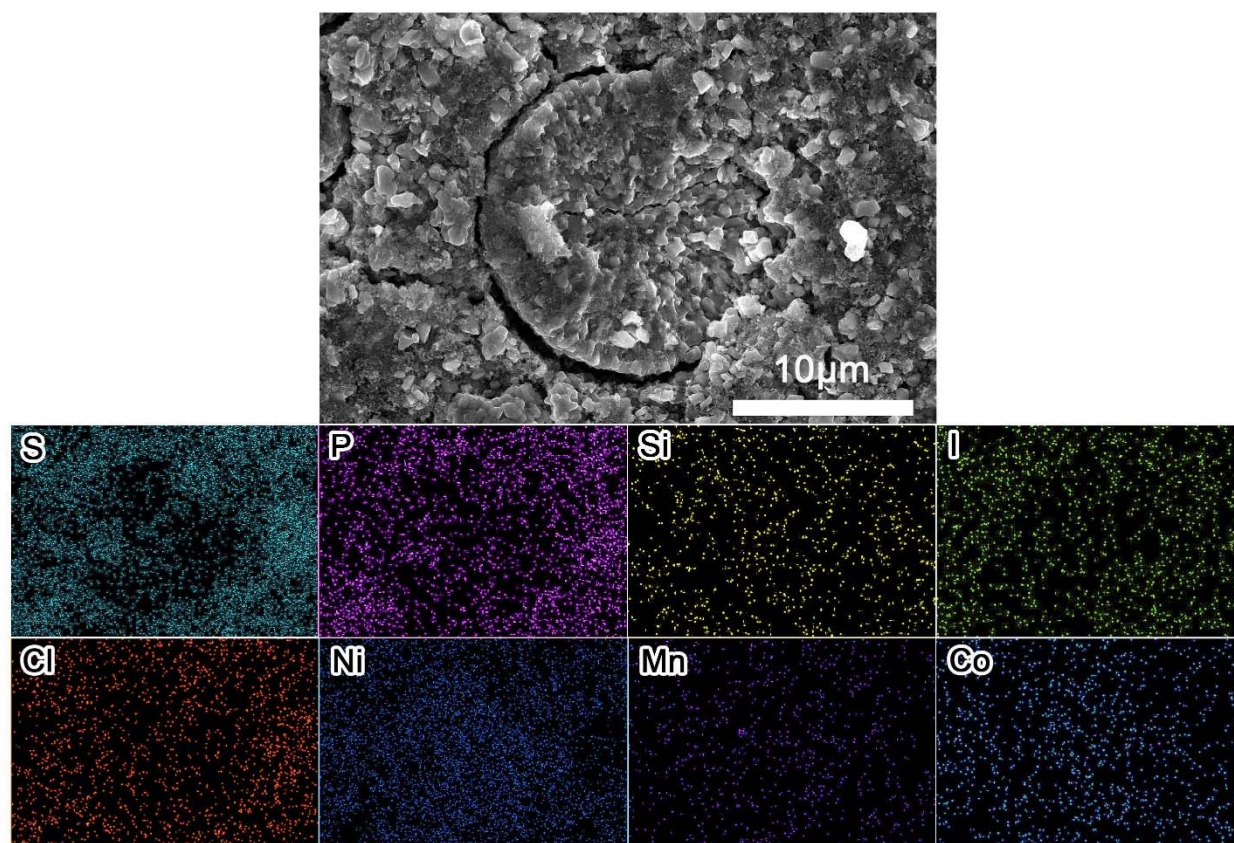


Figure S9. The SEM image and the corresponding elemental mappings of the cathode at the interface of $\text{Li}_{6.55}\text{P}_{0.45}\text{Si}_{0.55}\text{S}_5\text{I}$ SE/NCM.

Table S1. The extracted values of ionic conductivity and activation energy from Figure 3d.

x in $\text{Li}_{6+x}\text{P}_{1-x}\text{Si}_x\text{S}_5\text{I}$	Ionic conductivity (mS cm^{-1})	Activation energy (eV)
0	0.00023	0.73 / 0.76
0.1	0.0028	0.62 / 0.63
0.2	0.021	0.38 / 0.46
0.3	0.12	0.32
0.4	0.53	0.24
0.5	0.66	0.26
0.55	1.1	0.19
0.6	0.48	0.27